JOURNAL OF GEOPHYSICAL RESEARCH, VOL. 113, D14120, doi:10.1029/2008JD009901, 2008

Relationship between ENSO and northward propagating intraseasonal oscillation in the east Asian summer monsoon system

Kyung-Sook Yun,[1] Kyong-Hwan Seo,[1] and Kyung-Ja Ha[1]

Received 1 February 2008; revised 2 May 2008; accepted 14 May 2008; published 25 July 2008.

[1] Observational studies are presented on the relationship between El Niño–Southern Oscillation (ENSO) and the northward propagating intraseasonal oscillation (NPISO) in the east Asian summer monsoon (EASM) system. The summer NPISO activity shows a significant correlation with the preceding winter extreme phase of ENSO cycles. A higher correlation appears during late summer, which is consistent with frequent heavy rainfall events at that time as revealed in some previous case studies. The westward expansion of broad anticyclonic circulation over the western North Pacific and the smaller cyclonic circulation around Korea and Japan are found to be associated with the NPISO activity. ENSO affects the late summer NPISO activity through an atmospheric bridge and wave propagation; the springtime Indian Ocean sea surface temperature warming induced by ENSO through the Walker circulation leads to the downward motion and suppressed convection over the Philippine Sea, and this generates the forced Rossby wave train, forming the above south-to-north low-level circulation anomalies.

Citation: Yun, K.-S., K.-H. Seo, and K.-J. Ha (2008), Relationship between ENSO and northward propagating intraseasonal oscillation in the east Asian summer monsoon system, *J. Geophys. Res.*, *113*, D14120, doi:10.1029/2008JD009901.

1. Introduction

[2] The interannual variability of Asian summer monsoon (ASM) is dependent upon the seasonal mean structure and the intraseasonal oscillation (ISO). In particular, the ISO is known to determine the timing of the active and break periods of the ASM through the meridional movement of the monsoon trough [e.g., *Chen and Chen*, 1995], and consequently, the great damage to human activity and property is caused by sudden heavy precipitation, drought, and severe wind. Unlike the wintertime ISO (namely, the Madden and Julian Oscillation or the MJO), the boreal summer ISO exhibits an eastward propagation along the equator and a northwestward propagation in the Asian monsoon area [*Lau and Chan*, 1986; *Kemball-Cook and Wang*, 2001; *Seo et al.*, 2007]. The complexity in the boreal summer ISO may be explained by the development of an off-equatorial thermal equator, and thus asymmetric meridional sea surface temperature (SST) distribution relative to the equator [*Lawrence and Webster*, 2002].

[3] The boreal summer northward or northwestward propagating ISO (hereafter, referred to as NPISO) has been explained by the emanation of Rossby waves from enhanced deep convection in the Indian Ocean and western North Pacific [*Kemball-Cook and Wang*, 2001; *Hsu and Weng*, 2001; *Tsou et al.*, 2005; *Seo et al.*, 2007]. *Hsu and Weng* [2001] and *Seo et al.* [2007] have showed that the surface moisture convergence to the north of enhanced convection is the key factor for the NPISO. *Jiang et al.* [2004] have examined the relative roles of various internal dynamic mechanisms contributing to the northward propagation of the ISO convection. It is shown that a moisture convection feedback acts to develop the northward propagation in the tropical region (10°S–20°N), whereas a vertical easterly wind shear is more important in the off-equatorial region (north of 5°N). While most of the studies on the NPISO have focused on the tropical NPISO, *Krishnamurti and Gadgil* [1985] and *Kawamura et al.* [1996] have shown the existence of a significant extratropical NPISO variability with the period of about 30–60 days. *Tsou et al.* [2005] have demonstrated that the tropical ISO and extratropical ISO share a similar energy source. Furthermore, *Kawamura et al.* [1996] have found that the extratropical NPISO develops and propagates to the north when stronger convection occurs over the tropical western Pacific. The tropical convective activity is directly affected by large-scale circulation, which is in turn connected to El Niño–Southern Oscillation (ENSO).

[4] The relationships between the ENSO and the east Asian summer monsoon (EASM) on the interannual and interdecadal timescales have been previously studied by many researchers [*Wang and Li*, 1990; *Chang et al.*, 2000; *Wang et al.*, 2000]. Only *Teng and Wang* [2003] examined the contemporary relationship between developing ENSO during summer and the interannual variability of the summer NPISO in the tropical western North Pacific (WNP). Yet, a seemingly lagged relationship between ENSO and the NPISO has not been studied. Basically, because of a difficulty in relating phenomena on different timescales, the linkage between these two has not been explicitly investigated. Here, we attempt to investigate the relationship

[1]Division of Earth Environmental System, Pusan National University, Busan, South Korea.

0148-0227/08/2008JD009901$09.00

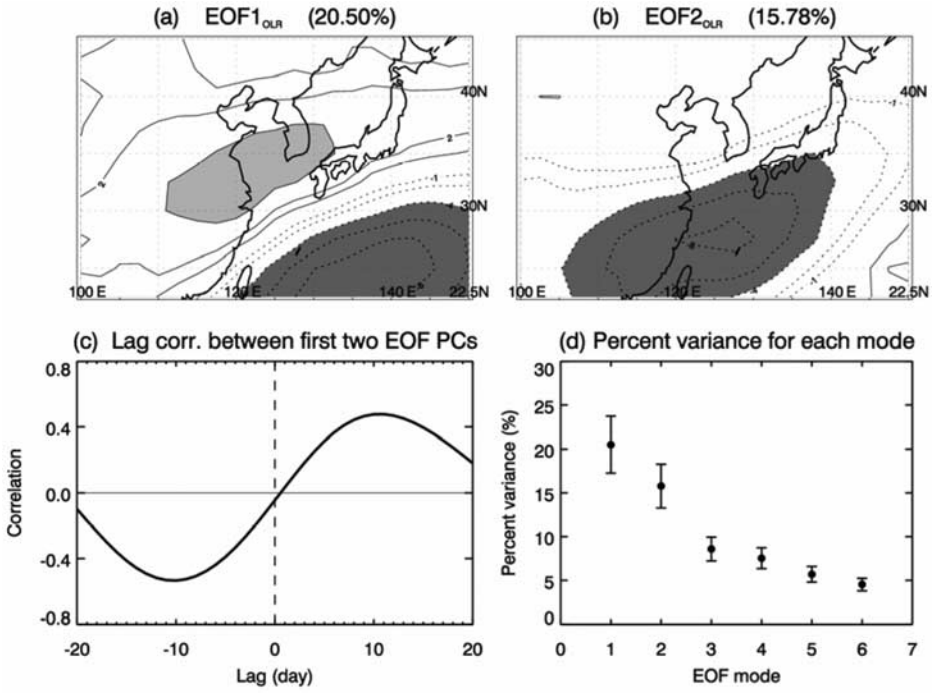

Figure 1. Spatial pattern of the (a) first and (b) second EOF modes obtained from 30 to 60 days filtered outgoing longwave radiation (OLR) data during extended summer (MJJASO) in 1979–2004. (c) The lag correlation coefficient between the principal component time series of the first two EOFs (PC1 and PC2). PC1 leads PC2. (d) Percent variance (%) explained by the first six EOF modes. The error bars represent the standard sampling errors on the basis of work by *North et al.* [1982].

between ENSO and the NPISO in the EASM, and its possible mechanisms. To this end, NPISO activity is estimated by the seasonal variance of the first two leading empirical orthogonal functions (EOFs) of convection. It will be shown that a westward expansion of the subtropical anticyclonic circulation over the WNP and Indian Ocean warming are associated with a significant, lagged ENSO-NPISO activity relationship.

2. Data and Methods

[5] To represent the ISO in the boreal summer, the daily outgoing longwave radiation (OLR) data from 1979 to 2004 obtained from NOAA (National Oceanic and Atmospheric Administration) are used. The seasonal cycle is first removed and anomaly fields are bandpass filtered to retain 30–60 days variability [*Lau and Chan*, 1986, *Tsou et al.*, 2005]. For the regressed dynamic fields, the NCEP/NCAR reanalysis data [*Kalnay et al.*, 1996] and HadISST (Hadley Centre Sea Ice and Sea Surface Temperature data set) [*Rayner et al.*, 2003] from 1979 to 2004 are also utilized. The monthly NINO SST indices from 1978 to 2005 are acquired from Climate Prediction Center/NOAA.

[6] The WNP monsoon and EASM have been known to exhibit a remarkable discontinuity in monsoonal flow and rainfall characteristics along ~22°N [*Wang and Ho*, 2002]. Therefore, the EASM domain is chosen as 100°–150°E and 22.5°–45°N and this domain well represents the EASM including Meiyu (China), Changma (Korea), and Baiu (Japan). To find the NPISO signal from extended boreal summer (that is, May 1st to October 31st) in the EASM region, an empirical orthogonal function (EOF) analysis of the bandpass filtered OLR data is applied. For this, the extended EOF method used by *Seo and Xue* [2005] has been also independently performed, but the results show similar northwestward propagating intraseasonal components (not shown). In this study, the NPISO is identified using the first two leading EOF modes and its activity is estimated by the variance of the principal component time series. To estimate slowly varying NPISO activity, a 91-day (or equivalently three-month) running average is applied to this NPISO activity. This provides the seasonal variance merging about two or three ISO events and thus an average ISO energy on the seasonal timescale. In this way, the two dominant oscillations with different timescales can be related and this approach has been previously used in studying the relationships between the wintertime MJO and ENSO by *Zhang and Gottschalck* [2002] and *Seo and Xue* [2005]. *Slingo et al.* [1996] have also used the seasonal ISO amplitude through a 100-day running mean. A three-month running average is also applied to NINO SST indices.

3. Relationship Between the NPISO Activity and ENSO

[7] As mentioned in section 2, the NPISO activity is defined as the variance of the first two EOF modes. The leading two EOFs generally appear as a pair, which together describe the large-scale propagating component [e.g., *Hendon et al.*, 1999]. Figures 1a and 1b display the first two EOF patterns of the intraseasonally filtered OLR. A

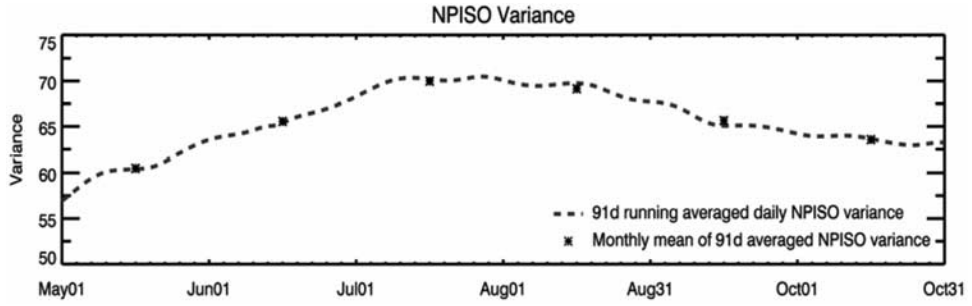

Figure 2. The temporal evolution of the 91-day running averaged daily NPISO variance and its monthly mean.

quadrature phase difference between the first two EOFs appears. The two principal component time series show significant correlations (over ~0.5) with a roughly 10-day lag (Figure 1c). According to the rule of thumb of *North et al.* [1982], the two EOF modes are statistically independent from the higher modes and contain the meaningful dynamical signal (Figure 1d). The higher EOF components are incoherent and noisy. It is shown from Figure 1 that the first two EOF modes represent the northwestward propagating ISO (NPISO) signal with about a 40-day period. The climatological distribution of 91-day running averaged NPISO variance (i.e., seasonal NPISO activity) and its monthly mean are shown in Figure 2. The NPISO activity exhibits the largest variance in July and August.

[8] To understand the relationship with ENSO, we calculate the correlation coefficient between the monthly NPISO activity during the extended summer (MJJASO) and the NINO3 (90°–150°W, 5°S–5°N) SST index with time lags from −24 to +24 month (Figure 3). In Figure 3, negative lag means that ENSO leads the NPISO activity and only coefficients significant at the 95% confidence level are shaded. A strong positive correlation is found during the months of July, August and September with the preceding winter NINO3 index, indicating that ENSO leads the NPISO in the EASM by about 7 to 11 months. Of particular interest is the appearance of the maximum relationship in August. While the NPISO itself exhibits the largest variance in July (Figure 2), the maximum correlation with ENSO occurs in August. Recent several case studies support the late summer maximum rainfall after strong El Niño events, such as a 1997–98 episode [*Yun et al.*, 2001; *Ha et al.*, 2005]. Note that the exclusion of the strongest 1997–98 ENSO warm event in the calculation of the lagged correlation only shows a negligible decrease of the peak correlation, suggesting the presence of a robust relationship. The use of the NINO3.4 index reveals the similar features to that shown above.

[9] The above relationship is manifested throughout the spatial regression of SST anomalies onto the NPISO activity in July–August (again, these are the months of the maximum relationship with ENSO) (Figure 4). During the preceding winter (DJF(−1)), the warm anomalies are apparent in the eastern Pacific. Meanwhile, in the Indian Ocean (the western Pacific), weak warm (cold) anomalies appear. The eastern Pacific warm anomalies moderately decay in the following spring (MAM0). The cold anomalies in the western Pacific persist through the spring season. Note that during this period, across the Indian Ocean, the basin-wide warming occurs and also warm anomalies appear over the South China Sea. This warming of the remote ocean basins after a warm ENSO event can be readily understood through a tropical atmospheric bridge process such as the Walker and Hadley circulations [*Klein et al.*, 1999; *Wang et al.*, 2006]. The vital role of the springtime Indian Ocean SST (IOSST) warming in the ENSO-NPISO activity relationship mentioned above is manifested in the subsequent analysis (refer to Figure 8). During the summer months (Figure 4c), the eastern Pacific warming is remarkably reduced and the warm anomalies over the Indian Ocean are weakened.

[10] To investigate how ENSO is connected with the NPISO activity in the EASM, regression analysis is performed for the 850-hPa geopotential height and vertically integrated moisture transport anomalies during the concur-

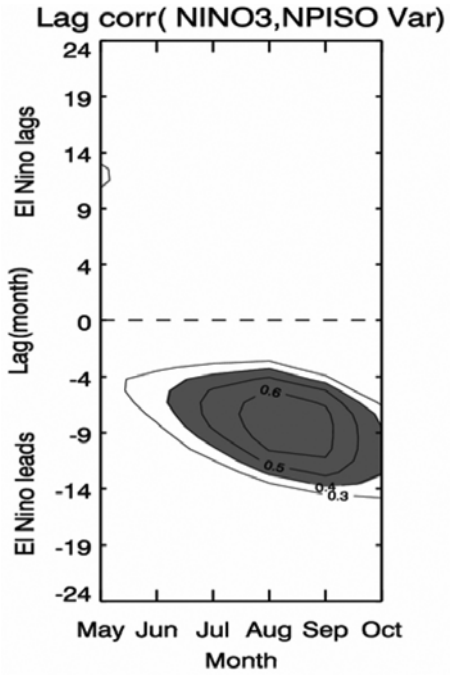

Figure 3. Lag lead correlation coefficients between the monthly NPISO activity for MJJASO and monthly NINO3 SST index. Only coefficients significant at the 95% confidence level are shaded.

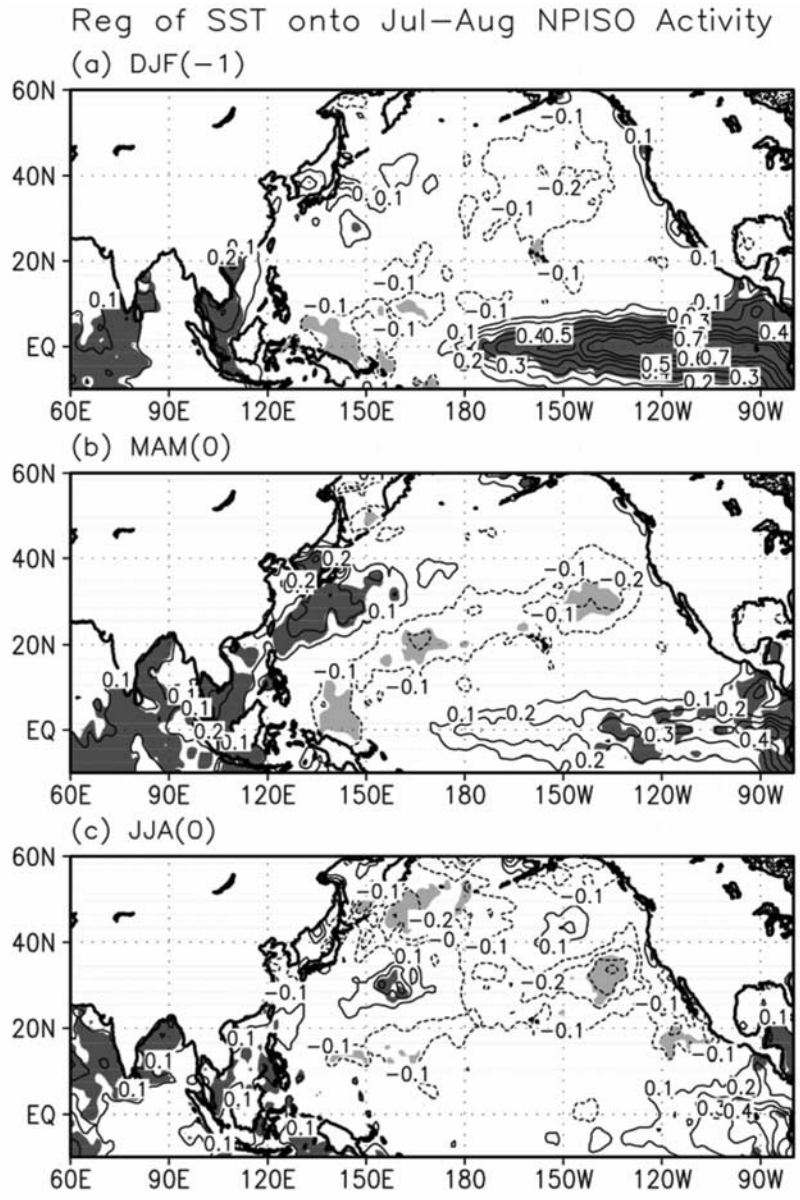

Figure 4. Regressed SST anomaly field against the July–August NPISO activity during (a) preceding winter (DJF), (b) MAM, and (c) JJA. Heavy (light) shading denotes positive (negative) SST anomalies significant at the 95% confidence level.

rent summer (JJA0) against the July–August NPISO activity (Figure 5). Immediately, we can see the broad anticyclonic anomalies in the WNP region (110°–180°E, 10°–30°N). This ridge is often referred to as the western North Pacific subtropical high (WNPSH) [e.g., *Lee et al.*, 2006]. Compared with the climatological distribution (shown as a thick line in Figure 5), the anomalous anticyclone is observed to have extended southwestward into the South China Sea. As the subtropical high intensifies with the westward extension along ~20°N, a smaller region of cyclonic anomalies appears to the north of this WNPSH. So along the western edge of the anticyclone, moisture is transported northward or northeastward into east Asia and is likely to converge into the low-pressure center located over Korea and Japan. Another high-pressure anomaly appears over the Okhotsk Sea. The low-level structure in northeast Asia is considerably similar to that shown in the positive phase of the EASM rainfall which is characterized by the tripole rainfall pattern in this area (i.e., more precipitation over central east China, Korea, and Japan) [*Hsu and Lin*, 2007], indicating the importance of the NPISO on the EASM rainfall.

[11] Now it is understood that the development of the strong NPISO activity is mainly related to the summertime WNP subtropical anticyclonic circulation and small cyclonic anomalies to the north. Thus, the relationship between ENSO and NPISO activity seen earlier might be associated with the low-level anticyclonic and cyclonic circulation anomalies over the WNP and northeast Asia. To see this, the summertime 850-hPa height anomalies are regressed against the peak ENSO phase (November–December–January) (Figure 6). The enhanced anticyclonic anomalies in the

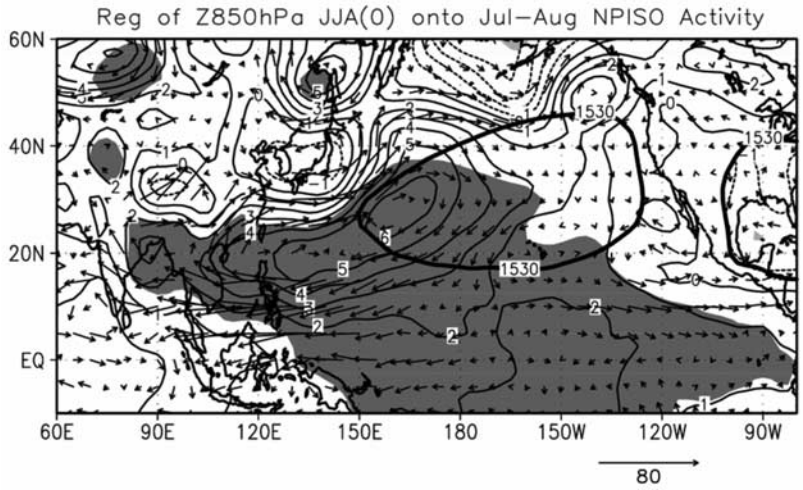

Figure 5. Regressed field for June–July–August 850-hPa geopotential height anomalies against the July–August NPISO activity. Thick solid line indicates the climatological 1530 m elevation of the 850-hPa geopotential height, and the arrows represent the vertically integrated anomalous moisture transport (kg m^{-1} s^{-1}). Heavy (light) shading denotes positive (negative) height anomalies significant at the 95% confidence level.

WNP and the Okhotsk Sea and the northern cyclonic anomalies are evident, similarly to Figure 5. Then a question remains as to how ENSO and the following summertime low-level circulation anomalies are related. Several studies have demonstrated the impact of ENSO on the WNPSH through the local air-sea interaction [e.g., *Wang et al.*, 2000; *Chang et al.*, 2000]. However, the regression analysis against the western Pacific SST anomalies does not show any systematic low-level height response (not shown), suggesting that the in situ SST forcing may not be a major factor for this ENSO-NPISO relationship. Instead, ENSO-related IOSST warming is considered as an important factor in the ENSO-NPISO relationship since the gradual basin wide warming in the Indian Ocean after the warm phase of ENSO is observed to occur in the following spring season through an atmospheric bridge process (Figure 4) and this affects the development of the WNPSH anomaly in the summer season [*Watanabe and Jin*, 2002; *Terao and Kubota*, 2005; *Yang et al.*, 2007]. The springtime Indian Ocean SST anomalies and preceding winter NINO3 index show a high correlation (~0.79). So, 850-hPa height anomalies are regressed against springtime Indian Ocean SST anomalies (averaged in the broad Indian Ocean ranging 20°S–20°N and 50°–100°E) (Figure 7). The regressed field exhibits a clear wave train structure along the east Asia coast with a remarkable similarity to that regressed to winter ENSO (Figure 6). This south-to-north three-cell circulation structure is also significantly similar to the pattern regressed against the July–August NPISO activity (Figure 5).

[12] The influence of the springtime IOSST warming on the summertime WNPSH can be explained by the convection activity over the western Pacific. To present this, OLR anomalies are regressed against the springtime IOSST anomaly component as in Figure 8a. Note that the IOSST

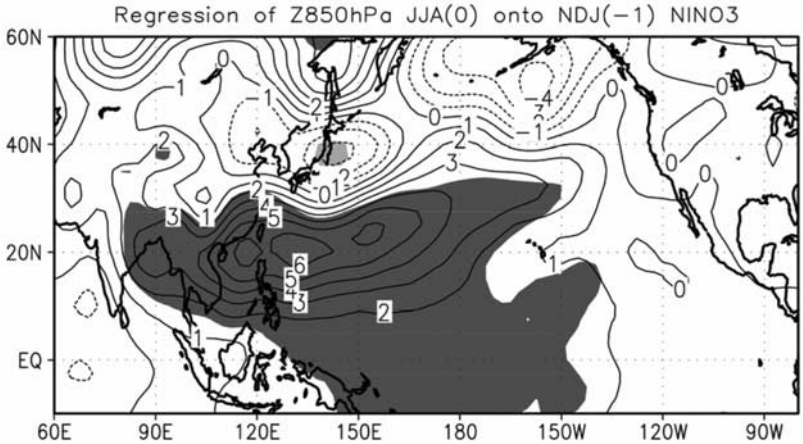

Figure 6. Regressed field for June–July–August 850-hPa geopotential height anomalies against November–December–January NINO3 SST index. Heavy (light) shading denotes positive (negative) height anomalies significant at the 95% confidence level.

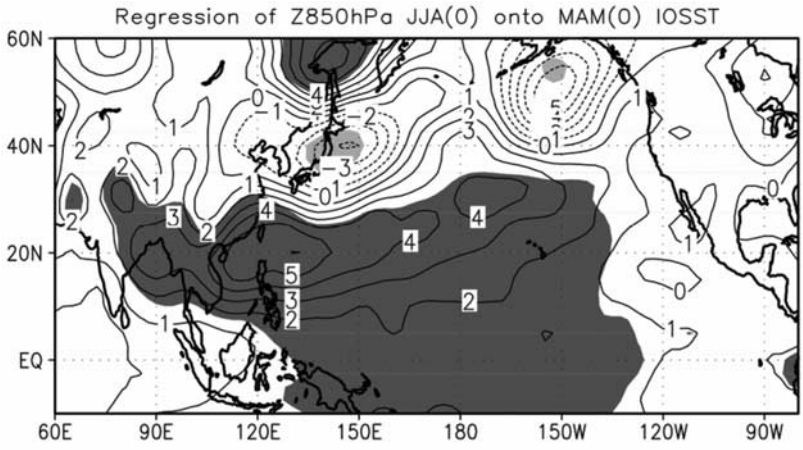

Figure 7. Regressed field for June–July–August 850-hPa geopotential height anomalies against March–April–May Indian Ocean SST anomalies averaged over (20°S–20°N, 50°–100°E). Heavy (light) shading denotes positive (negative) height anomalies significant at the 95% confidence level.

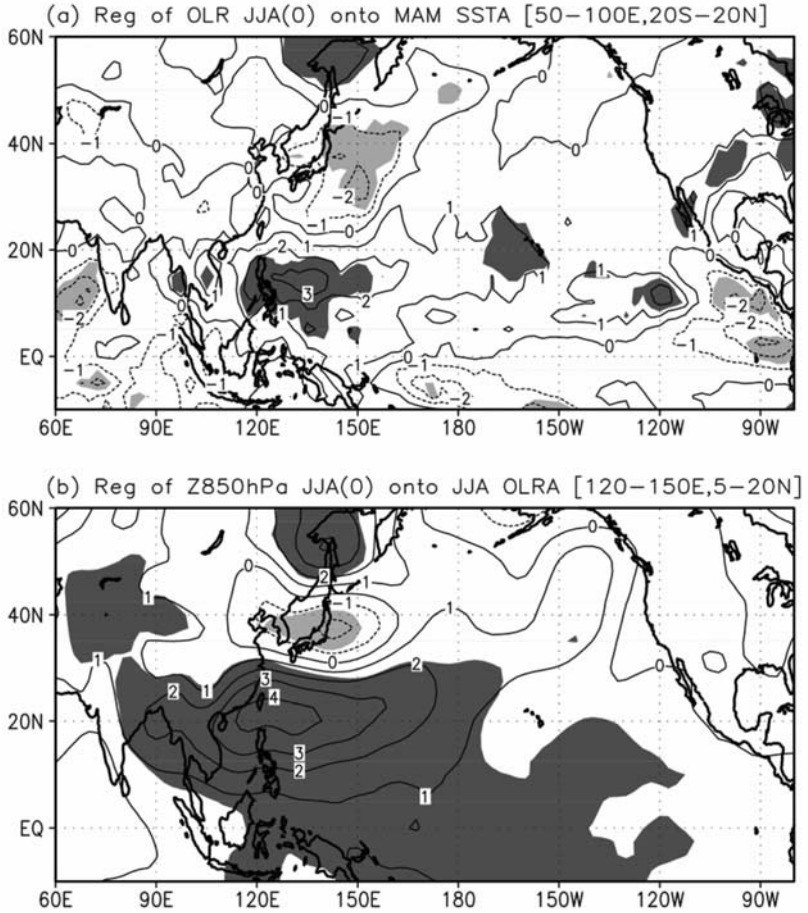

Figure 8. (a) June–July–August OLR anomalies regressed against March–April–May Indian Ocean SST anomalies averaged over (20°S–20°N, 50°–100°E). The MAM IOSST anomalies are extracted beforehand by regressing onto the July–August NPISO activity. (b) June–July–August 850-hPa geopotential height anomalies regressed against June–July–August OLR anomalies averaged over (5°–20°N, 120°–150°E). The JJA OLR anomalies are extracted beforehand by regressing onto the July–August NPISO activity. Shading denotes anomalies significant at the 95% confidence level.

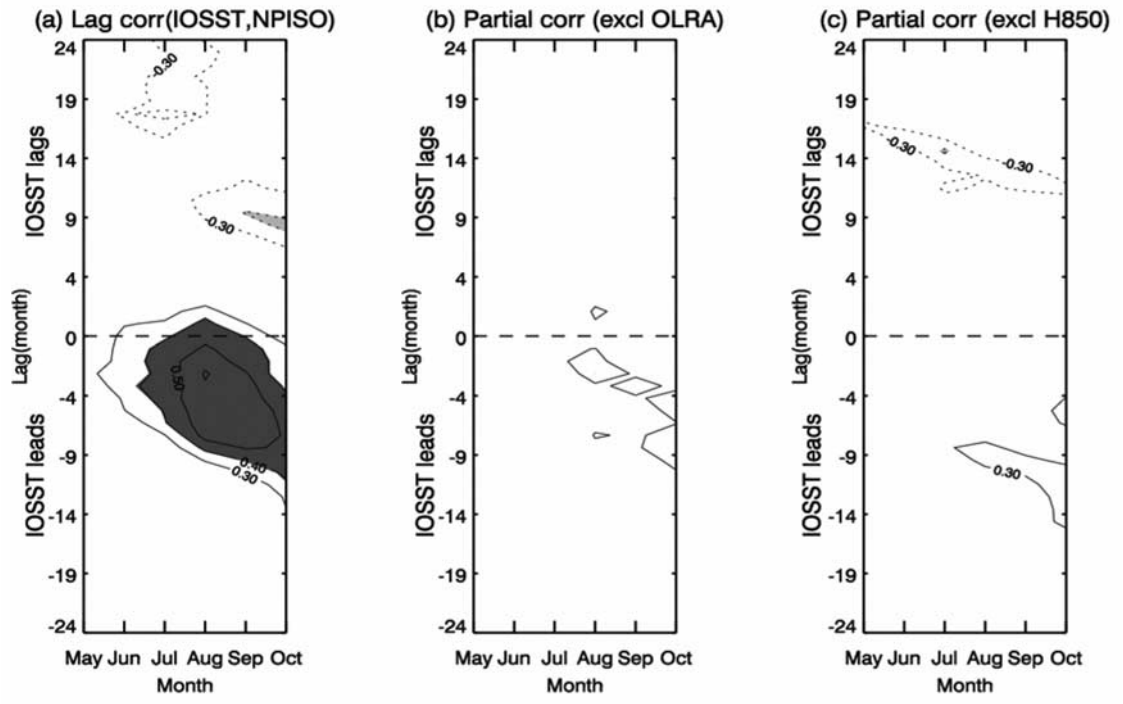

Figure 9. (a) Lag lead correlation coefficients between the monthly NPISO activity for MJJASO and monthly IOSST anomalies. (b) The partial correlation between the monthly NPISO activity for MJJASO and monthly IOSST anomalies excluding the effect of June–July–August OLR anomalies averaged over (5°–20°N, 120°–150°E). (c) Same as in Figure 9b, but for excluding the 850-hPa geopotential height anomalies averaged over (15°–25°N, 120°–180°E). Only coefficients significant at the 95% confidence level are shaded.

anomaly used in Figure 8a is calculated with the component that is linearly related to the July–August NPISO activity (i.e., this component has been obtained in advance by regression onto the NPISO activity). The regression of OLR anomalies directly onto the original IOSST anomaly field also exhibits the wave-like structure similar to the above. In Figure 8a, the regressed field shows suppressed convection over the Philippine Sea and enhanced convection to the east of Japan and west of the Indian subcontinent. On the other hand, the SST forcing over the Maritime Continent is not responsible for the wavelike circulation structure in the extratropical region. The regressed OLR field against the summertime SST anomalies over the Maritime Continent shown in Figure 4c shows enhanced convection over the Maritime Continent and suppressed convection over the central Pacific (not shown), not representing the previous three-cell structure along the east Asia coast.

[13] Notice that the suppressed convection anomaly over the Philippine Sea is strongest in Figure 8a. This convection anomaly over the Philippine Sea has been attributed to a weakened Walker circulation due to the downward motion in the western Pacific [*Lee et al.*, 2006]. The reversed Walker circulation (that is, the upward motion in the Indian Ocean and downward motion in the WNP) is also seen in the regressed vertical velocity against the July–August NPISO activity (not shown). The WNP downward motion is evidently strongest during the summer season, consistent with the development of suppressed convection over the Philippine Sea.

[14] Then, the summertime 850-hPa height fields are regressed onto a time series that represents the strength of this suppressed convection (i.e., JJA OLR anomaly averaged over 120°–150°E and 5°–20°N) (Figure 8b). The convection anomalies have been also extracted beforehand by regressing onto the July–August NPISO activity. It shows a remarkably similar south-to-north wave train structure to that seen in Figure 5 with a high pressure over the WNP, low pressure over Korea and Japan and another small high over the Okhotsk Sea, although the location and magnitude of the respective centers are slightly different. In particular, the geopotential height anomaly over the extratropical eastern North Pacific shows a somewhat different structure between Figure 5, Figure 7 and Figure 8b. It may be attributed to a local effect or mixed wave origins. That is, the eastern North Pacific region is affected by the local vorticity forcing and the Rossby wave train originated from both the WNP and the upstream Eurasian continent along the Asian jet [*Hsu and Lin*, 2007]. The strength of the regressed WNPSH is ~70% of that regressed directly onto the July–August NIPSO activity (Figure 5). The WNPSH occurs to the northwest of the suppressed convection anomaly, consistent with a Gill-type Rossby wave response to reduced heating. It is remarkably consistent with the work by *Lu and Dong* [2001], which shows that the suppressed convection over the warm pool is related to the westward extension of the WNPSH. More importantly, the suppressed convection induces a strong wave train extending from the WNP along the east Asian coast,

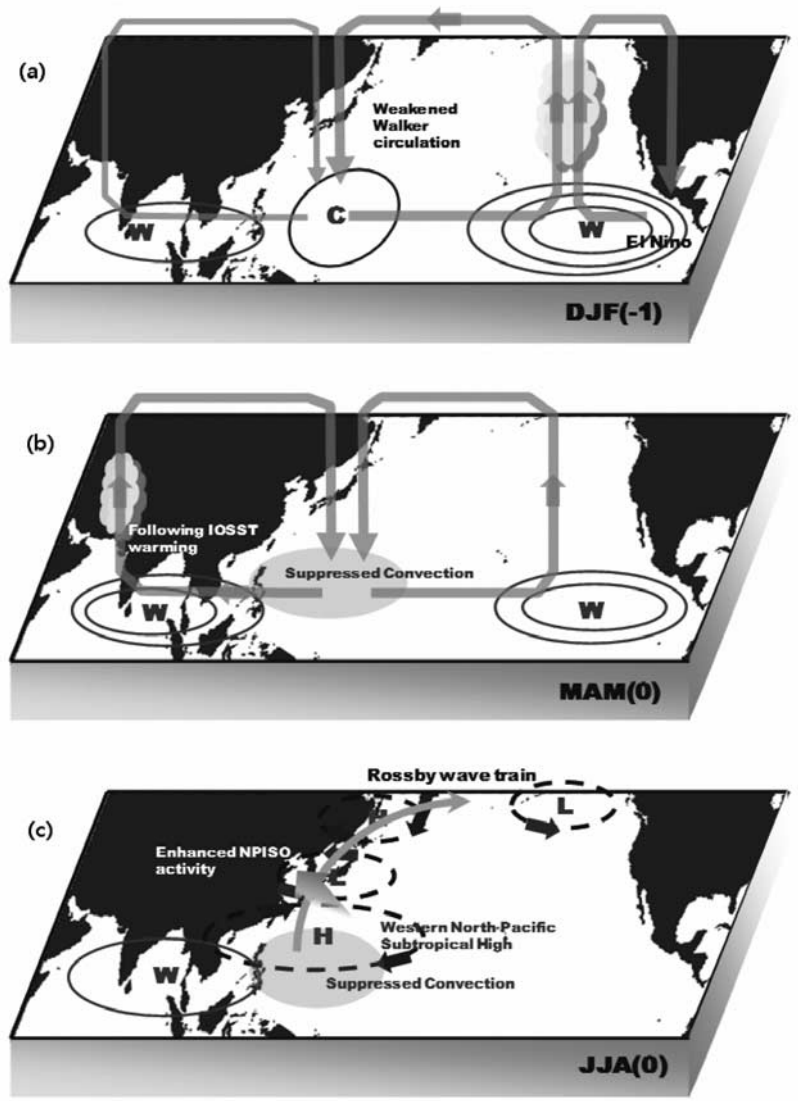

Figure 10. The schematic diagram showing the seasonal sequence of the ENSO-NPISO relationship during (a) DJF(−1), (b) MAM(0), and (c) JJA(0).

resembling the east Asia-Pacific (EAP) [*Huang and Lu*, 1989] or Pacific-Japan (PJ) pattern [*Nitta*, 1987].

[15] As mentioned in the previous results, the springtime IOSST warming plays an important role in developing the summertime NPISO activity. Figure 9a shows the lagged correlation between the monthly NPISO activity and IOSST anomalies. This confirms that the springtime IOSST warming is closely linked to the July–August NPISO activity. As another way to look at the importance of the western Pacific convection and WNPSH in the relationship between the NPISO and IOSST warming, a partial correlation coefficient is calculated (Figures 9b and 9c). The partial correlation is the linear correlation of two variables after the linear relationships between these two variables and another third variable are removed. So if a partial correlation is approximately equivalent to zero, it is considered that the two variables are strongly dependent upon the third variable. When either the effect of the western Pacific convection activity or WNPSH (averaged in the area ranging 15°–25°N, 120°–180°E) is removed, the partial correlation does not show any significant signals. This means that the significant connection between the springtime IOSST warming and boreal summer NPISO in the EASM is through the western Pacific convection activity and WNPSH. Therefore, the springtime IOSST warming leads to the downward circulation and suppressed convection over the WNP region during the summer period. This induces the WNPSH and the midlatitude low-pressure anomalies with the latter producing enhanced rainfall over China, Korea, and Japan. In summary, ENSO is related to the late summer NPISO activity through the Indian Ocean warming (via the Walker circulation induced by warm ENSO episode) and the WNPSH and cyclonic circulation anomalies over the northeast Asia (via the stationary Rossby wave train forced by the downward motion and suppressed convection in the western Pacific along ∼15°N). The relationship between ENSO and the WNPSH in boreal

summer is also supported by modeling study of *Li et al.* [2007].

4. Summary and Discussion

[16] The relationship between ENSO and the northwestward propagation of the 30–60 day intraseasonal oscillation (NPISO) in the EASM region has been explored. The boreal summer NPISO activity shows a statistically significant correlation with the preceding winter extreme phase of the ENSO cycle. The maximum correlation appears during late summer, implying the possible association with frequent heavy rainfall events in east Asia. This strong late summer relationship is because during early summer, the EASM is mainly controlled by the monsoonal frontal system, but after late July, east Asia is largely influenced by the subtropical anticyclonic circulation [*Ueda et al.*, 1995; *Lim et al.*, 2002]. Therefore, the dynamical effect of the WNP subtropical high can be larger in late summer, which actually tends to connect the NPISO and ENSO. This relationship is illustrated in a schematic diagram in Figure 10. During the preceding winter, strong warming takes place over the eastern/central Pacific (that is, El Niño). It induces a modest warming in the Indian Ocean and weak cooling in the western Pacific through the weakened Walker circulation (Figure 10a). The Indian Ocean warming induces downward circulation and suppressed convection anomalies over the Philippine Sea (Figure 10b). This, in turn, acts to generate a Rossby wave train, and consequently the summertime low-level subtropical anticyclonic circulation anomaly in the WNP (WNPSH) and cyclonic circulation anomaly around Korea and Japan (Figure 10c). Therefore, ENSO appears to indirectly affect the late summer NPISO activity through a tropical atmospheric bridge process and Rossby wave propagation, not through the local SST forcing. The previous study showing the existence of statistically significant relationship between the IOSST and WNPSH by *Gong and Ho* [2002] supports our hypothesis.

[17] Although this paper does not specifically explain which component of the dynamical mechanisms is most important (e.g., Indian Ocean SST, Pacific SST, downward motion and convection anomalies over the Pacific, air-sea interaction, teleconnection, and local versus remote SST effects), it may contribute to the understanding of the overall relationship between ENSO and EASM and especially the dynamic connection of the two different timescale oscillations (i.e., ENSO and ISO) because the current general circulation models (GCMs) are unable to simulate the proper ISO variability in boreal summer and the possible relationship with ENSO. An appropriate simulation of the summertime ISO in GCMs and its sensitivity tests are a challenging task. Last, a preliminary result shows that a significant lagged correlation exists between the ISO activity of the Indian monsoon and ENSO with the former leading the latter in early summer. The detailed dynamical processes will be explored in the future.

[18] **Acknowledgments.** We would like to thank Soon-Il An for his constructive comments. This work was supported by the Ministry of Environment as "The Eco-Technopia 21 Project"and Korea Research Foundation grant funded by the Korean Government (MOEHRD) (KRF-2007-313-C00783).

References

Chang, C.-P., Y. Zhang, and T. Li (2000), Interannual and interdecadal variations of the east Asian summer monsoon and tropical Pacific SSTs. Part I: Roles of the subtropical ridge, *J. Clim.*, *13*, 4310–4325, doi:10.1175/1520-0442(2000)013<4310:IAIVOT>2.0.CO;2.

Chen, T.-C., and J.-M. Chen (1995), An observational study of the South China Sea monsoon during the 1979 summer: Onset and life cycle, *Mon. Weather Rev.*, *123*, 2295–2318, doi:10.1175/1520-0493(1995)123<2295:AOSOTS>2.0.CO;2.

Gong, D.-Y., and C.-H. Ho (2002), Shift in the summer rainfall over the Yangtze River valley in the late 1970s, *Geophys. Res. Lett.*, *29*(10), 1436, doi:10.1029/2001GL014523.

Ha, K.-J., S.-K. Park, and K.-Y. Kim (2005), On interannual characteristics of Climate Prediction Center merged analysis precipitation over the Korean peninsula during the summer monsoon season, *Int. J. Climatol.*, *25*, 99–116, doi:10.1002/joc.1116.

Hendon, H. H., C. Zhang, and J. D. Glick (1999), Interannual variation of the Madden-Julian Oscillation during austral summer, *J. Clim.*, *12*, 2538–2550.

Hsu, H.-H., and S.-M. Lin (2007), Asymmetry of the tripole rainfall pattern during the east Asian summer, *J. Clim.*, *20*, 4443–4458, doi:10.1175/JCLI4246.1.

Hsu, H.-H., and C.-H. Weng (2001), Northwestward propagation of the intraseasonal oscillation in the western North Pacific during the boreal summer: Structure and mechanism, *J. Clim.*, *14*, 3834–3850, doi:10.1175/1520-0442(2001)014<3834:NPOTIO>2.0.CO;2.

Huang, R.-H., and L. Lu (1989), Numerical simulation of the relationship between the anomaly of the subtropical high over east Asia and the convective activities in the western tropical Pacific, *Adv. Atmos. Sci.*, *6*, 202–214, doi:10.1007/BF02658016.

Jiang, X., T. Li, and B. Wang (2004), Structures and mechanisms of the northward propagating boreal summer intraseasonal oscillation, *J. Clim.*, *17*, 1022–1039, doi:10.1175/1520-0442(2004)017<1022:SAMOTN>2.0.CO;2.

Kalnay, E., et al. (1996), The NCEP/NCAR 40-year reanalysis project, *Bull. Am. Meteorol. Soc.*, *77*, 437–471, doi:10.1175/1520-0477(1996)077<0437:TNYRP>2.0.CO;2.

Kawamura, R., T. Murakami, and B. Wang (1996), Tropical and mid-latitude 45-day perturbations over the western Pacific during the northern summer, *J. Meteorol. Soc. Jpn.*, *74*, 867–890.

Kemball-Cook, S., and B. Wang (2001), Equatorial waves and air-sea interaction in the boreal summer intraseasonal oscillation, *J. Clim.*, *14*, 2923–2942, doi:10.1175/1520-0442(2001)014<2923:EWAASI>2.0.CO;2.

Klein, S. A., B. J. Soden, and N.-C. Lau (1999), Remote sea surface temperature variations during ENSO: Evidence for a tropical atmospheric bridge, *J. Clim.*, *12*, 917–932, doi:10.1175/1520-0442(1999)012<0917:RSSTVD>2.0.CO;2.

Krishnamurti, T. N., and S. Gadgil (1985), On the structure of the 30 to 50 day mode over the globe during FGGE, *Tellus, Ser. A*, *37*, 336–360.

Lau, K.-M., and P.-H. Chan (1986), Aspects of the 40–50 day oscillation during the northern summer as inferred from outgoing longwave radiation, *Mon. Weather Rev.*, *114*, 1354–1367, doi:10.1175/1520-0493(1986)114<1354:AOTDOD>2.0.CO;2.

Lawrence, D. M., and P. J. Webster (2002), The boreal summer intraseasonal oscillation: Relationship between northward and eastward movement of convection, *J. Atmos. Sci.*, *59*, 1593–1606, doi:10.1175/1520-0469(2002)059<1593:TBSIOR>2.0.CO;2.

Lee, E.-J., S.-W. Yeh, J.-G. Jhun, and B.-K. Moon (2006), Seasonal change in anomalous WNPSH associated with the strong east Asian summer monsoon, *Geophys. Res. Lett.*, *33*, L21702, doi:10.1029/2006GL027474.

Li, Y., R.-Y. Lu, and B.-W. Dong (2007), The ENSO-Asian monsoon interaction in a coupled ocean-atmosphere GCM, *J. Clim.*, *20*, 5164–5177, doi:10.1175/JCLI4289.1.

Lim, Y.-K., K.-Y. Kim, and H.-S. Lee (2002), Temporal and spatial evolution of the Asian summer monsoon in the seasonal cycle of synoptic fields, *J. Clim.*, *15*, 3630–3644, doi:10.1175/1520-0442(2002)015<3630:TASEOT>2.0.CO;2.

Lu, R.-Y., and B.-W. Dong (2001), Westward extension of North Pacific subtropical high in summer, *J. Meteorol. Soc. Jpn.*, *79*, 1229–1241, doi:10.2151/jmsj.79.1229.

Nitta, T. (1987), Convective activities in the tropical western Pacific and their impact on the northern hemisphere summer circulation, *J. Meteorol. Soc. Jpn.*, *65*, 373–390.

North, G. R., T. L. Bell, F. J. Moeng, and R. F. Cahalan (1982), Sampling errors in the estimation of empirical orthogonal functions, *Mon. Weather Rev.*, *110*, 699–706, doi:10.1175/1520-0493(1982)110<0699:SEITEO>2.0.CO;2.

Rayner, N. A., D. E. Parker, E. B. Horton, C. K. Folland, L. V. Alexander, D. P. Rowell, E. C. Kent, and A. Kaplan (2003), Global analyses of sea surface temperature, sea ice, and night marine air temperature since the

late nineteenth century, *J. Geophys. Res.*, *108*(D14), 4407, doi:10.1029/2002JD002670.

Seo, K.-H., and Y. Xue (2005), MJO-related oceanic Kelvin waves and the ENSO cycle: A study with the NCEP Global Ocean Data Assimilation System, *Geophys. Res. Lett.*, *32*, L07712, doi:10.1029/2005GL022511.

Seo, K.-H., J.-K. E. Schemm, W. Wang, and A. Kumar (2007), The boreal summer intraseasonal oscillation simulated in the NCEP Climate Forecast System: The effect of sea surface temperature, *Mon. Weather Rev.*, *135*, 1807–1827, doi:10.1175/MWR3369.1.

Slingo, J. M., et al. (1996), Intraseasonal oscillation in 15 atmospheric general circulation models: Results from an AMIP diagnostic subject, *Clim. Dyn.*, *12*, 325–357, doi:10.1007/BF00231106.

Teng, H., and B. Wang (2003), Interannual Variations of the boreal summer intraseasonal oscillation in the Asian-Pacific region, *J. Clim.*, *16*, 3572–3584, doi:10.1175/1520-0442(2003)016<3572:IVOTBS>2.0.CO;2.

Terao, T., and T. Kubota (2005), East-west SST contrast over the tropical oceans and the post El Nino western North Pacific summer monsoon, *Geophys. Res. Lett.*, *32*, L15706, doi:10.1029/2005GL023010.

Tsou, C.-H., P.-C. Hsu, W.-S. Kau, and H.-H. Hsu (2005), Northward and northwestward propagation of 30–60 day oscillation in the tropical and extratropical western North Pacific, *J. Meteorol. Soc. Jpn.*, *83*, 711–726, doi:10.2151/jmsj.83.711.

Ueda, H., T. Yasunari, and R. Kawamura (1995), Abrupt seasonal change of large-scale convective activity over the western Pacific in the northern summer, *J. Meteorol. Soc. Jpn.*, *73*, 795–809.

Wang, B., and L. Ho (2002), Rainy season of the Asian-Pacific summer monsoon, *J. Clim.*, *15*, 386–398, doi:10.1175/1520-0442(2002)015<0386:RSOTAP>2.0.CO;2.

Wang, B., R. Wu, and X. Fu (2000), Pacific-east Asian teleconnection: How does ENSO affect east Asian climate?, *J. Clim.*, *13*, 1517–1536, doi:10.1175/1520-0442(2000)013<1517:PEATHD>2.0.CO;2.

Wang, C., W. Wang, D. Wang, and Q. Wang (2006), Interannual variability of the South China Sea associated with El Niño, *J. Geophys. Res.*, *111*, C03023, doi:10.1029/2005JC003333.

Wang, W.-C., and K. Li (1990), Precipitation fluctuation over semiarid region in northern China and the relationship with El Niño/Southern Oscillation, *J. Clim.*, *3*, 769–783, doi:10.1175/1520-0442(1990)003<0769:PFOSRI>2.0.CO;2.

Watanabe, M., and F.-F. Jin (2002), Role of Indian Ocean warming in the development of Philippine Sea anticyclone during ENSO, *Geophys. Res. Lett.*, *29*(10), 1478, doi:10.1029/2001GL014318.

Yang, J., Q. Liu, S.-P. Xie, Z. Liu, and L. Wu (2007), Impact of the Indian Ocean SST basin mode on the Asian summer monsoon, *Geophys. Res. Lett.*, *34*, L02708, doi:10.1029/2006GL028571.

Yun, W.-T., C.-K. Park, J.-W. Lee, H.-S. Lee, and S.-K. Min (2001), Analysis of the Korea heavy rainfall feature in summer 1998, *J. Korean Meteorol. Soc.*, *37*(2), 181–194.

Zhang, C., and J. Gottschalck (2002), SST anomalies of ENSO and the Madden-Julian Oscillation in the equatorial Pacific, *J. Clim.*, *15*, 2429–2445, doi:10.1175/1520-0442(2002)015<2429:SAOEAT>2.0.CO;2.

K.-J. Ha, K.-H. Seo (corresponding author), and K.-S. Yun, Division of Earth Environmental System, Atmospheric Science, Pusan National University, Busan 609-735, South Korea. (khseo@pusan.ac.kr)